CONF-970585--1

LA-UR- 96-4597

Structural Characterization and Comparision of Iridium, Platinum and Gold/Palladium Ultra-Thin Film Coatings for STM of Biomolecules.

R. Sebring[1], P. Arendt[1], J. Panitz[4], P. Yau[3], B. Imai[2], E.M. Bradbury[2] and J. Gatewood[2]

RECEIVED
FEB 14 1997
OSTI

[1]*Material Sciences Division and* [2]*Life Sciences Division, Los Alamos National Laboratory, Los Alamos, New Mexico 87545*
3 Dept of Biological Chemistry, School of Medicine, U.C. Davis, California , 95616
4 Dept. Physics and Astronomy, University of New Mexico, Albuquerque, New Mexico 87131

Key Words. Cathode sputtering, ion-beam sputtering, gold/palladium, platinum, iridium, metal film, STM, TEM, HOPG .

MASTER

Summary

Scanning tunnelling microscopy (STM) is capable of atomic resolution and is ideally suited for imaging surfaces with uniform work function. A biological sample on a conducting substrate in air does not meet this criteria and requires a conductive coating for stable and reproducible STM imaging. In this paper, we describe the STM and transmission electron microscopy (TEM) characterization of ultra-thin ion-beam sputtered films of iridium and cathode sputtered gold/palladium and platinum films on highly ordered pyrolytic graphite (HOPG) which were developed for use as biomolecule coatings.

Our goals were the development of metal coatings sufficiently thin and fine grained that 15-20 Å features of biological molecules could be resolved using STM, and the development of a substrate/coating system which would allow complementary TEM information to be obtained for films and biological molecules. We demonstrate in this paper that ion-beam sputtered iridium on highly ordered pyrolytic graphite (HOPG) has met both these goals.

The ion-beam sputtered iridium produced a very fine grained (< 10 Å) continuous film at 5-6 Å thickness suitable for stable air STM imaging. In comparison, cathode sputtered platinum produced 16 Å grains with the thinnest continuous film at 15 Å thickness, and the sputtered gold/palladium produced 25 Å grains with the thinnest continuous film at 18 Å thickness.

Introduction

The high resolution topographic capabilities of the STM (Binnig and Rohrer, 1983) are of direct application in addressing many biological structure questions. Unfortunately, imaging a typical biological molecule, such as DNA, by STM has proven difficult. Reproducible results have

DISTRIBUTION OF THIS DOCUMENT IS UNLIMITED

DISCLAIMER

This report was prepared as an account of work sponsored by an agency of the United States Government. Neither the United States Government nor any agency thereof, nor any of their employees, make any warranty, express or implied, or assumes any legal liability or responsibility for the accuracy, completeness, or usefulness of any information, apparatus, product, or process disclosed, or represents that its use would not infringe privately owned rights. Reference herein to any specific commercial product, process, or service by trade name, trademark, manufacturer, or otherwise does not necessarily constitute or imply its endorsement, recommendation, or favoring by the United States Government or any agency thereof. The views and opinions of authors expressed herein do not necessarily state or reflect those of the United States Government or any agency thereof.

DISCLAIMER

Portions of this document may be illegible in electronic image products. Images are produced from the best available original document.

been obtained for DNA in liquid electrochemical cells (Lindsay *et al.*, 1992) but a conductive coating is required for STM imaging of DNA in air (Dunlap *et al.*, 1993). These coatings should have the following characteristics: electrically conductive, provide a uniform work function, be physically and chemically stable air, extremely fine grained and very thin.

Thermally evaporated films of C, Pt/C and Pt/C/Ir have been used as coatings for STM of biological molecules (Wilkins *et al.*, 1993; Stemmer *et al.*, 1989; Buhle *et al.*, 1985; Gross *et al.*, 1985; Amrein *et al.*, 1989; Zasadzinski *et al.*, 1988; Wepf *et al.*, 1991; Guckenberger *et al.*, 1988;).

Sputter coating has been shown to offer advantages over thermal evaporation. Sputtered atoms have a higher kinetic energy than evaporated atoms (Peters, 1986) and are more likely to bind to the substrate. Consequently, the resulting film is more uniform and provides a better geometrical representation of the surface (Wildhaber *et al.*, 1985; Gross *et al.*, 1985; Winkler *et al.*, 1985; Studer *et al.*, 1981). In addition, the minimum thickness required for a continuous film is reduced (Wildhaber *et al.*, 1985).

Ion-beam sputtered films have been shown to be more uniform and have finer grain size than cathode sputtered films (Kemmenoe & Bullock, 1983, Newbury *et al.*, 1988). Ion-beam sputtered Pt has produced 10-12 Å grains (Kemmenoe & Bullock, 1983) as opposed to larger 17 Å grains for cathode sputtered films.

Our goals were the development of metal coatings sufficiently thin and fine grained that 15-20 Å features of biological molecules could be resolved using STM, and the development of a substrate/coating system which would allow complementary TEM information to be obtained for films and biological molecules. We demonstrate in this paper that ion-beam sputtered iridium on highly ordered pyrolytic graphite (HOPG) has met both these goals.

Materials And Methods

HOPG substrate preparation

For STM substrates, a block (1 cm sq. by 3 mm deep) of HOPG (ZYA Union Carbide) was attached to an aluminum SEM stub with colloidal graphite and a fresh surface was prepared immediately prior to the experiment by cleaving with adhesive tape in the usual manner.

High resolution TEM imaging required ultra-thin (< 30 Å) HOPG substrates. A flake was cleaved from the STM bulk HOPG (see above) with adhesive tape. With the tape still attached, the flake was glued (Itoya O'Glue, Torrance, Ca.) to a tungsten TEM grid with the tape side facing away from grid. After the glue dried, the HOPG was again cleaved by grasping the grid with one pair of tweezers and the tape with another and

pulling the two apart from each other. This resulted in a very thin, nearly transparent film of HOPG adhered to the glue surface on the grid. The thick layer of glue holding the HOPG to the grid was subsequently removed by floating the grid, cleaved surface away from water, on nano-pure distilled water. As the glue dissolves, the grid would invariably release from the HOPG and sink to the bottom of the petri dish leaving the HOPG floating on the water surface. This HOPG flake was picked up from below the water surface with a clean TEM grid and refloated on clean water in another petri dish. Since the HOPG flake at this stage is only a millimeter square or less and nearly transparent it is best to perform these steps while viewing through a low power stereo microscope. This "washing" procedure was repeated 10 times and after the final wash, the flake was picked up one last time on a clean TEM grid and air dried. The result of this procedure is an HOPG substrate which has one freshly cleaved surface that has not been in direct contact with any water solutions. and is suitably thin enough for high resolution TEM darkfield analysis. All HOPG substrates were prepared and used the same day.

Cathode Sputtered Gold-Palladium and Platinum Films

Cathode sputtering was performed in an oil diffusion pumped vacuum evaporator (Denton DV 502). equipped with a liquid nitrogen baffle. Au/Pd (60:40) or Pt targets were pre-sputtered directly prior to film depositon to remove surface contaminants. The bell jar was purged 3 times with research grade argon (Air Products Tamaqua, Pa) and the samples sputtered (Denton DSM-5A cool magnetron sputter coater) at 60 mtorr Argon pressure for 5 seconds with Au/Pd, or 4 seconds with Pt at a plasma discharge current of 20 mA and a target to specimen distance of 12 cm..

Ion-Beam Sputter Coating of Iridium

The iridium films were produced in a cryo-pumped vacuum system equipped with a 2.5 cm diameter ion sputter deposition gun (Ion Tech Inc., Fort Collins, Co). Prior to deposition, the system was pumped to a base pressure of 8.7×10^{-5} torr. The ion-beam current and voltage operating parameters were 50 mA and 700 volts, respectively. The target was 99.999% pure iridium and was positioned 15 cm from the HOPG substrates. The ion gun, target and substrates were positioned such that the deposition would be perpendicular to the sample surface.

Biological Samples

Nucleosomes were isolated from chicken erythrocyte nuclei by digestion with micrococcal nuclease followed by H1 / H5 depletion of the solubilized chromatin. The solubilized H1 / H5 depleted chromatin was redigested with micrococcal nuclease until only core particles and traces of dimer

remained. The redigested chromatin was purified by 5-20 % sucrose gradient centrifugation. 0.5 ml fractions, which contained either pure core particles or largely dinucleosomes were dialyzed against a 1000 X excess of cross-linking buffer (10 mM Triethanolamine HCL, pH 8.0, 25 mM NaCl) overnight, followed by 100 ml of 2% glutaraldehyde in cross-linking buffer overnight and 3 x 100 ml of cross-linking buffer over three days.

Ferritin, horse spleen, cationized molecules (Polysciences, Inc.) were used fresh, as received from Polysciences, without any fixation or dilution.

A 5 µl solution containing biological molecules was applied directly onto the HOPG surface for 3 minutes; briefly washed with nano-pure water and then air dried. All biological samples for STM imaging were further cathode or ion-beam sputter coated.

TEM operation

Samples were analyzed using a Philips 410 transmission electron microscope equipped with a liquid nitrogen cold finger anti-contamination device and a LaB6 filament. Brightfield and high resolution conical darkfield images were imaged with 100 kv accelerating voltage and photographed at a nominal magnification of 65,000. Brightfield images were recorded at Scherzer defocus conditions. If the HOPG substrate crystal diffraction artifacts seriously interfered with the specimen image, the crystal was tilted a few degrees from the 0001 plane until they were minimized. All images were made from single crystal regions of the HOPG as determined by selected area electron diffraction. Regions that were too thick to provide suitable darkfield contrast or large numbers of crystal defects were avoided. TEM magnification was calibrated with a high magnification carbon grating (Ladd Res. Ind.).

Thickness measurements of sputtered metal films was determined by TEM using a technique in which the sputtered film is visualized on the surface of 100 nm diameter gold spheres as described by Johansen (1984) .

STM operation

Scanning tunneling microscopy was performed under ambient conditions in air using a commercial STM (Park Scientific Instruments) operated in constant current mode with mechanically clipped probe tips of Pt/Ir, 80/20, 0.5 mm dia. wire (Alfa Research Chemicals). The bias voltage was generally positive but negative bias voltages showed no observable difference. Tunneling conditions were 0.5-0.7 volts with a tunneling current of 0.1-0.2 nA. The majority of tips provided suitable resolution of the metal film particles. When a tip became contaminated as observed by image smearing or multiple imaging, the tip was occasionally recovered by "conditioning" with a brief pulse of 2-3 volts. This would generally not show any damage to the substrate, but if higher voltage pulses (>5 volts)

were required, this would damage the substrate by punching a 5-10 nm diameter hole in the coating down to the graphite substrate. If the tip could not be recovered by the above method, it was replaced with a new tip. All STM imaging of Au/Pd or Pt films was performed within the same day the samples were prepared. Ir coated samples were usually produced in the afternoon and kept under vacuum until they were imaged the following day. Coatings that were to be directly compared with each other were prepared and imaged consecutively with the same STM tip under identical tunneling conditions. The data were collected at a scan rate of 1-5 Hz/scan line at 256 pixel image resolution. All images were corrected for tilt in the x direction by fitting a first or second order polynomial to an averaged x line of all the x lines in the image and then subtracting this polynomial from each horizontal line in the data. STM x - y calibration was based on the known lattice constants of HOPG.

3. Results

Cathode sputtered Au/Pd and Pt films

Discontinuous films of Au/Pd or Pt are not suitable due to instability during scanning. We experimentally determined the minimum stable coating thickness for each type of film by generating a series of films in which we gradually decreased the amount of deposited metal until the film became unstable in the STM experiment. The instability was evidenced by removal of metal clusters during repeated scans of the same area. The minimum coating thickness required for stable tunnelling on Pt and Au/Pd films on HOPG was determined to be 15 and 18 Å respectively. The Au/Pd films could be rescanned successfully for up to 1 week and the Pt films for up to 3 days.

Characteristic minimum thickness films are shown in Figure 1 for Au/Pd (A-C) and Pt (D-F). STM images (A and D, Bar= 1000 Å: B and E, bar= 100 Å) show closely packed particles. The particles appear smaller and less packed in the TEM (C and F, bar = 100 Å). Upon close inspection of the TEM images, phase noise is apparent in the intervening space between the strongly contrasted particles. Image analysis of several hundred TEM imaged particles showed that the mean equivalent circular diameter ± 1 s.d. of the Pd/Au particles was 25 ± 10 Å and the Pt particles was 16 ± 4 Å. Our results agree with the Au/Pd particles size of 23±10 Å reported by Echlin (1981) and 16±4 Å for Pt particles reported by Kemmenoe & Bullock (1983). After completion of this study, Pt was chosen as the most suitable metal for cathode sputtering and was used for all subsequent experiments utilizing this sputter approach.

Ion-beam sputtered Ir films

The time series designed to determine the minimum coating thickness required for stable Ir films is shown in Figure 2. The sputter times were 2 minutes (A and B), 1 minute (C and D), 30 seconds (E and F), and 15 seconds (G and H) with film thicknesses of 22 Å, 15 Å, 9 Å and approximately 5 Å. STM images are shown in A,C,E, and G and the corresponding TEM images are shown in B, D, F, and H. The 5 Å thick film proved to be stable for STM. TEM images of the 15 Å Ir film resemble the Au/Pd and Pt images, showing highly contrasted particles with intervening spaces. The 9 Å and 5 Å thick film TEM images are essentially all phase noise but high resolution darkfield TEM imaging of the 5 Å film resolved very fine particles of 6-10 Å dimension (Figure 2, I). The Ir ion-beam sputtered films were more susceptible to air exposure than either the Au/Pd or Pt cathode sputtered films. The best STM results were obtained when the Ir films were scanned with 24 hours of air exposure.

Coating of biomolecules

The height profiles for the biomolecules we study using STM range from approximately 5 Å to 60 Å. In order to determine if the sputter coatings would remain stable when contouring a biological molecule, we coated ferritin molecules with Pt or Ir and imaged using STM. Cathode sputtered Pt coatings at ~20 Å thickness and ion-beam sputter coatings of Ir at ~7 Å thickness were stable. The STM results are shown in Figure 3. The Pt coated ferritin molecules (A, ~160 Å dia.) were larger than the Ir coated ferritin (B, ~145 Å). This size difference is consistent with the difference in coating thickness. The diameter of ferritin less coating (~140 Å d) is larger than the 130 Å diameter previously reported (Massover, 1993) while the heights (60-85 Å) are less. This observation is consistent with a flattening of the unfixed molecules, but may also be influenced by STM calibration. The z axis calibration is based on single graphite steps and is not well suited for molecules with this height profile. This calibration method may introduce error in the z measurements.

STM of Pt and Ir coated DNA-histone core particles was a direct comparison utilizing the same core particle sample imaged in the STM on the same day with the same tip under identical tunnelling conditions. Two size classes of particles were visible in the Ir coated sample. The size of the Pt coated particles (C, ~145 Å d) is again greater than the size of the Ir coated particles (D, ~126 Å d), consistent with the difference in coating thickness. The diameter of the larger particles less coating (~112 Å) is consistent with the value determined by solution neutron scattering (110 Å, Imai *et al.*, 1986) and X-ray crystallography (Richmond *et al.*, 1984). The height (~33 Å) is lower than the expected 55 Å which may be due to calibration errors (see above) or molecule flattening. The smaller particles are oblate (~70 Å x 100 Å) with dimensions similar to DNA depleted histone octamers (70 Å x 110 Å, Burlingame *et al.*, 1985).

4. Discussion

We have demonstrated that cathode sputtered Au/Pd and Pt on HOPG can be used to produce very thin, continuous, stable coatings for STM in air. By using HOPG as a substrate, we achieved for STM the minimum coating thickness and small particle size previously achieved for electron microscopy (Echlin, 1981; Kemmenoe & Bullock, 1983). This contrasts with the 100-150 Å thick Au/Pd films required for stable tunneling on mica substrate (Mantovani *et al.*, 1990; Kemmenoe & Bullock, 1983). The superior ion-beam sputtered Ir on HOPG has potential as a high resolution coating for air STM of biological samples.

Cathode sputtering utilizes conventional equipment found in most electron microscopy laboratories and commercially available metal targets of suitable purity. The relative rarity of ultra pure iridium targets and ion-

beam equipment limits the routine use of ion-beam sputter coatings. Our strategy is to use cathode sputtered Pt to characterize sample binding properties, contamination levels, etc. and then apply ion-beam sputtered Ir in the final stages of sample analysis. We expect this combined approach to yield high resolution STM images of biomolecules with minimal expense.

5. References

Amrein, M., Dürr, R., Winkler, H., Travaglini, G., Wepf, R. & Gross, H. (1989) STM of freeze-dried and Pt-Ir-C-coated bacteriophage T4 Polyheads. *J. Ultrastruct. Res.* **102**, 170-177.

Binnig, G. & Rohrer, H. (1983) Scanning tunneling microscopy. *Surf. Sci.* **126**, 236-244.

Buhle, E.L.Jr., Aebi, U. & Smith P.R., (1985) Correlation of surface topography of metal-shadowed specimens with their negatively stained reconstructions. *Ultramicroscopy* **16**, 436-450.

Burlingame, R.W., Love, W.E., Wang, B.C., Hamlin, R., Xuong, N.G., and Moudrianakis, E.N. (1985) *Science* **228**, 546-553.

Dunlap, D.D., Garcia, R., Schabtach, E., and Bustamante, C. (1993), Masking generates contiguous segments of metal-coated and bare DNA for scanning tunnelling microscope imaging., *PNAS* (USA), **90(16)**, 7652-7655.

Echlin, P. (1981) Recent advances in specimen coating techniques. *Scanning Electron Microscopy* 1981, **I**, 79-90. SEM Inc., AMF O'Hare, Ill.

Gross, H., Müller, T., Wildhaber, I. & Winkler, H. (1985) High resolution metal replication, quantified by image processing of periodic test specimens. *Ultramicroscopy* **16**, 287-304.

Guckenberger, R, Wiegräbe, W. & Baumeister, W. (1988) Scanning tunneling microscopy of biomacromolecules. *J. of Microsc.* **152**, 795-802.

Imai, B.S., Yau, P., Baldwin, J.P., Ibel, K., May, R.P., and Bradbury, E.M. (1986), Hyperacetylation of core histones does not cause unfolding of nucleosomes., *J. Biol. Chem.*, **261(19)**, 8784-8792.

Johansen, B.V. & Namork, E. (1984) Sputtered platinum films on colloidal gold particles: a calibration specimen for quartz film thickness monitors. *J. Microsc.* **133**, 83-87.

Kemmenoe, B.H. & Bullock, G.R. (1983) Structure analysis of sputter-coated and ion-beam sputter-coated films: a comparative study. *J. Microsc.* **132**, 153-163.

Lindsay, S.M., Tao, N.J., DeRose, J.A., Oden, P.I., Lyubchenko, Yu, L., Harrington, R.E., and Shlyakhtenko, L. (1992), Potentiostatic deposition of DNA for scanning probe microscopy., *Biophys*, J., **61**, 1570-1584.

Mantovani, J.G., Allison, D.P., Warmack, R.J., Ferrell, T.L., Ford, J.R., Manos, R.E., Thompson, J.R., Reddick, B.B. & Jacobson, K.B. (1990) Scanning tunneling microscopy of tobacco mosaic virus on evaporated and sputter-coated palladium / gold substrates. *J. Microsc.* **158**, 109-116.

Massover, W.H (1993). Ultrastructure of Ferritin and Apoferritin: A Review. *Micron*, **24 (4)**, 389-437.

Newbury, D.E., Joy, D.C., Echlin, P., Fiori, C.E. & Goldstein, J.I. (1988) *Advanced scanning electron microscopy and X-ray microanalysis*. 295-448. Plenum Press.

Peters, K.R. (1986) Rationale for the application of thin, continuous metal films in high magnification electron microscopy. *J. Microsc.* **142**, 25-34.

Richmond, T.J., Finch, J.T., Rushton, B., Rhodes, D., and Klug, A. (1984). Structure of nucleosome core particles at 7 Å resolution., *Nature*, **311**, 532-537.

Stemmer, A., Hefti, A., Aebi, A. & Engel, A. (1989) Scanning tunneling and transmission electron microscopy on identical areas of biological specimens. *Ultramicroscopy* **30**, 263-280.

Studer, D., Moor, H. & Gross, H. (1981) Single bacteriorhodopsin molecules revealed on both surfaces of freeze-dried and heavy metal-decorated purple membranes. *J. Cell Biol.* **90**, 153-159.

Wepf, R., Amrein, M., Bürkli, U. & Gross H. (1991) Platinum/iridium/carbon: a high-resolution shadowing material for TEM, STM and SEM of biological marcromolecular structures. *J. Microsc.* **163**, 51-64.

Wildhaber, I., Gross, H. & Moor, H. (1985) Comparative studies of very thin shadowing films produced by atom beam sputtering and electron beam evaporation. *Ultramicroscopy* **16**, 321-330.

Wilkins, M.J., Davies, M.C., Jackson, D.E., Mitchell, J.R., Roberts, C.J., Stokke, B.T. & Tendler, S.J.B. (1993) Comparison of scanning tunneling microscopy and transmission electron microscopy image data of microbial polysaccharide. *Ultramicroscopy* **48**, 197-201.

Winkler, H., Wildhaber, I. & Gross, H. (1985) Decoration effects on the surface of a regular protein layer. *Ultramicroscopy* **16**, 331-339.

Wood, M.J., Yau, P., Imai, B.S., Goldberg, M.W., Lambert, S.J., Fowler, A.G., Baldwin, J.P., Godfrey, J.E., Moudrianakis, E.N., Koch, M.H.J., Ibel, K., May, R.P., and Bradbury, E.M. (1991), Neutron and X-ray scatter studies of the histone octamer and amino and carboxyl domain trimmed octamers., *J. Biol.l Chem.* **266 (9)**, 5696-5702.

Zasadzinski, J.A.N., Schneir, J., Gurley, J., Elings, V., & Hansma, P.K. Scanning tunneling microscopy of freeze-fracture replicas of biomembranes. *Science* **239**, 1014-1016.

FIGURE LEGENDS

Fig. 1. A series of STM and TEM micrographs of low voltage, magnetron cathode sputtered Au/Pd (15 Å film thickness) and Pt (18 Å film thickness) on HOPG. A) STM of Au/Pd, Bar = 1000 Å. (B) STM of Au/Pd, Bar = 100 Å (C) TEM of Au/Pd, Bar = 100 Å. (D) STM of Pt, Bar = 1000 Å. (E) STM of Pt, Bar = 100 Å (F) TEM of Pt, Bar = 100 Å. The grains in the TEM images appear to be individual particles, each with a light phase ring around the particle and separated by a space. The STM images of the same films appear as closely packed spherical particles.

Fig. 2. A series of STM and bright field TEM micrographs of ion-beam sputtered iridium deposited on HOPG at decreasing film thicknesses by varying the ionbeam sputter time from 2 minutes to 15 seconds. All images are printed at the same magnification to facilitate comparisons. (A) STM 22 Å film thickness, (B) TEM 22 Å film thickness, (C) STM 15 Å film thickness, (D) TEM 15 Å film thickness, (E) STM 9 Å film thickness, (F) TEM 9 Å film thickness, (G) STM 5-6 Å film thickness, (H) TEM 5-6 Å film thickness. (I) High resolution conical darkfield of 5-6 Å film thickness showing discrete particles not resolved in (H). The grain size and roughness of the film decreases with decreasing film thickness. Bars = 100 Å

Fig. 3. STM images of Pt coated (~20 Å film thickness) and Ir coated (~5 Å film thickness) ferritin molecules and DNA-histone nucleosomes. (A) Pt coated ferritin. (B) Ir coated ferritin. (C) Pt coated nucleosomes. (D) Ir coated nucleosomes. The arrows in A and B point to individual ferritin molecules. The Ir coated molecules appear smaller than the same molecules coated with Pt. Note the Z axis scale in B is 100 Å compared to 200 Å in A.

Fig. 1

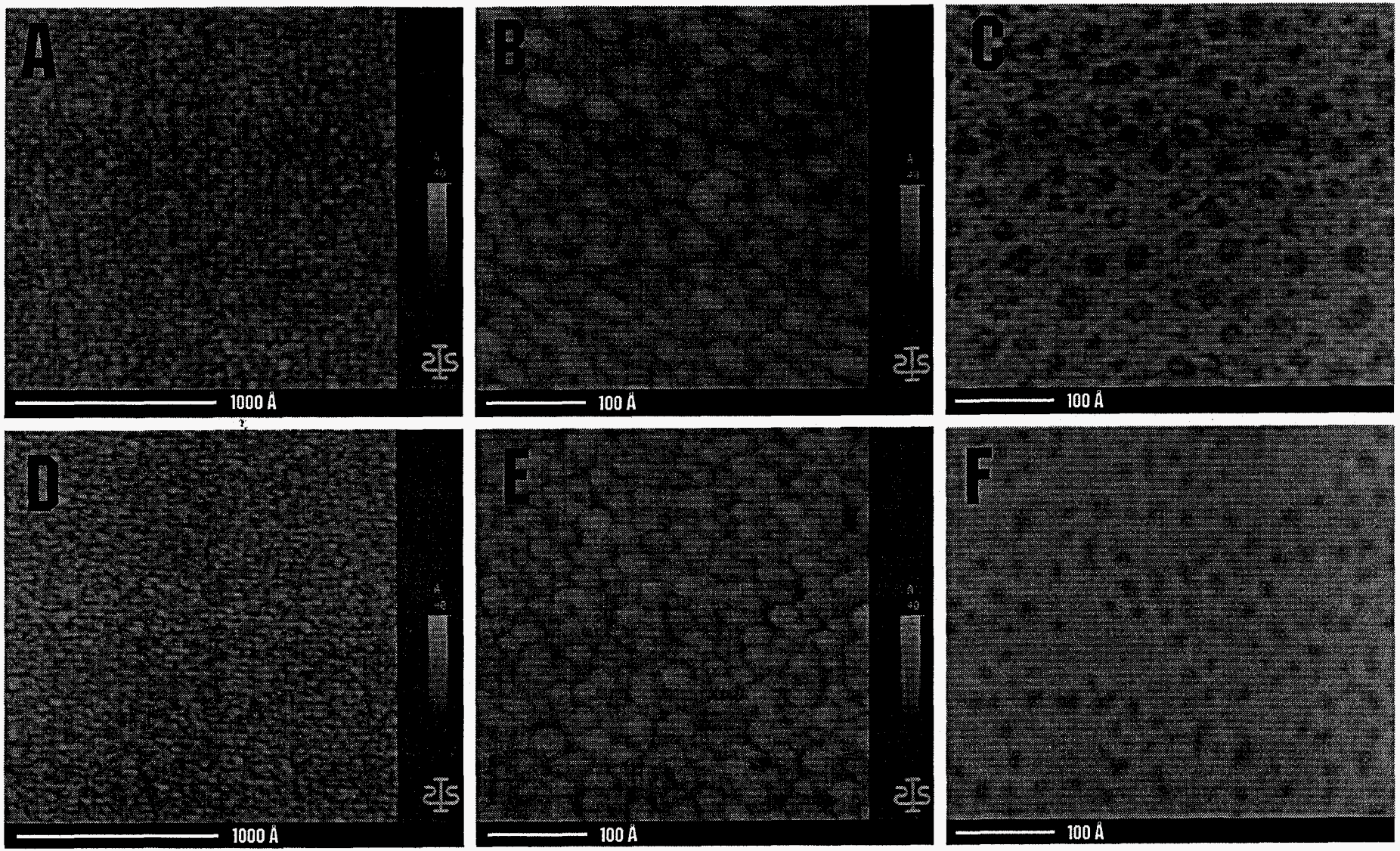

Fig. 2

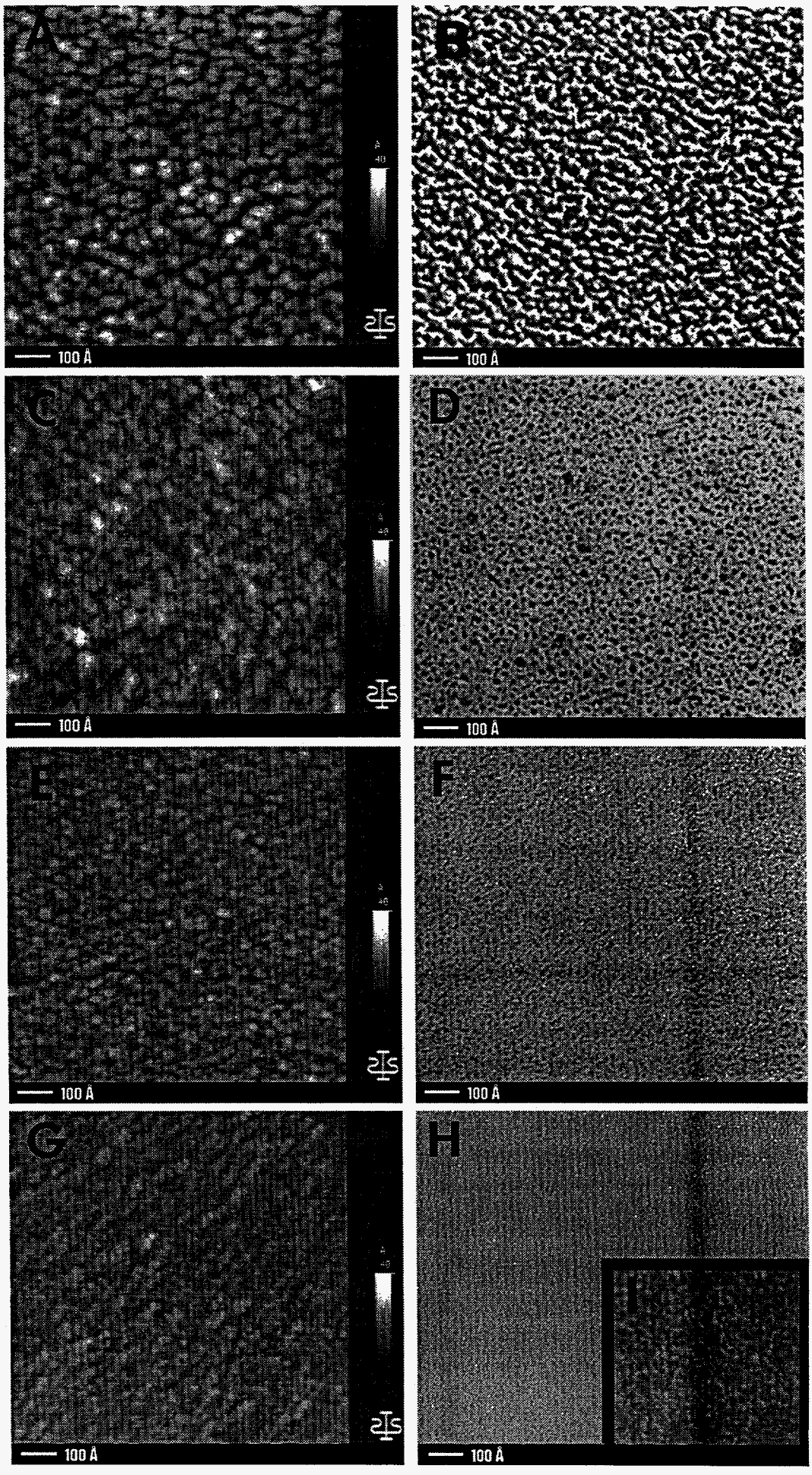

Fig. 5